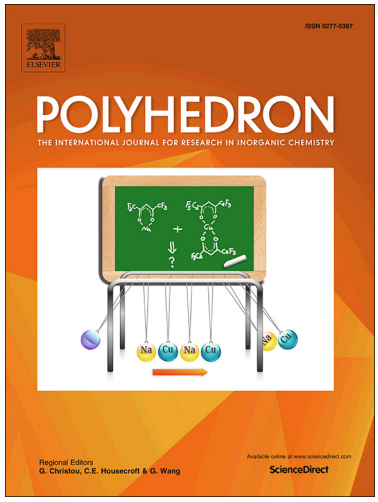

Synthesis and structures of copper(II) complexes containing *N*,*N*-bidentate *N*-substituted phenylethanamine derivatives as pre-catalysts for heterotactic-enriched polylactide

Juhyun Cho, Min Kyung Chun, Saira Nayab, Jong Hwa Jeong

PII: S0277-5387(19)30107-X
DOI: https://doi.org/10.1016/j.poly.2019.02.014
Reference: POLY 13758

To appear in: *Polyhedron*

Received Date: 10 December 2018
Revised Date: 7 February 2019
Accepted Date: 8 February 2019

Please cite this article as: J. Cho, M. Kyung Chun, S. Nayab, J. Hwa Jeong, Synthesis and structures of copper(II) complexes containing *N*,*N*-bidentate *N*-substituted phenylethanamine derivatives as pre-catalysts for heterotactic-enriched polylactide, *Polyhedron* (2019), doi: https://doi.org/10.1016/j.poly.2019.02.014

Revised

Synthesis and structures of copper(II) complexes containing *N*,*N*-bidentate *N*-substituted phenylethanamine derivatives as pre-catalysts for heterotactic-enriched polylactide

Juhyun Cho, Min Kyung Chun, Saira Nayab[a], Jong Hwa Jeong*

[a] *Department of Chemistry and Green-Nano Materials Research Center, Kyungpook National University, 1370 Sankyuk-dong, Taegu,702-701, Republic of Korea.*
[b] *Department of Chemistry, Shaheed Benazir Bhutto University, Sheringal, Dir (Upper), Khyber Pakhtunkhwa, Islamic Republic of Pakistan.*

---

*Corresponding author. Tel: +82-53-950-6343; fax: +82-53-950-6330

E-mail address: *jeongjh@knu.ac.kr*

Synthesis and structures of copper(II) complexes containing *N*,*N*-bidentate *N*-substituted phenylethanamine derivatives as pre-catalysts for heterotactic-enriched polylactide

Juhyun Cho, Min Kyung Chun, Saira Nayab[a], Jong Hwa Jeong*

[a] *Department of Chemistry and Green-Nano Materials Research Center, Kyungpook National University, 1370 Sankyuk-dong, Taegu,702-701, Republic of Korea.*

[b] *Department of Chemistry, Shaheed Benazir Bhutto University, Sheringal, Dir (Upper), Khyber Pakhtunkhwa, Islamic Republic of Pakistan.*

Abstract

A series of Cu(II) complexes, $[L^nCuCl_2]_2$ (L^n = (*S*)-*N*-((1H-pyrazol-1-yl)methyl)-1-phenylethanamine (L^1), (*S*)-*N*-((3,5-dimethyl-1H-pyrazol-1-yl)methyl)-1-phenylethanamine (L^2) and (*S*)-1-phenyl-*N*-((pyridin-2-yl)methyl)ethanamine (L^3)) were synthesised and characterised. X-ray diffraction analysis revealed that the molecular structures of these distorted square planar Cu(II) complexes were dimeric with two asymmetric units crystallised in the (S_C, S_N) and (S_C, R_N) configurations. These are rare examples of dimeric Cu(II) complexes. The alkoxide derivatives, generated *in situ*, catalysed the ring-opening polymerisation of *rac*-lactide in a controlled fashion and displayed high activities (2 or 3 min for complete conversion).

Heterotactic-enriched polylactide (with P_r up to 0.86) was formed using these initiators at room temperature in CH_2Cl_2.
Keywords: Copper complexes, Heterotactic-enriched polylactide, Ring-opening polymerisation, Single-site catalysts, X-ray structure

1. Introduction

Depleting petroleum resources and the accumulation of plastics in the environment favours the use of bio-renewable and biodegradable polymers. Polylactide (PLA), a biodegradable and biocompatible polymer, has attracted interest because lactide (monomer) can be obtained from natural resources and does not depend directly on fossil fuels [1-4]. Using organometallic complexes as initiators *via* the ″coordination-insertion mechanism″ is the preferred route to PLAs because the products have high number average molecular weights (M_n) and low polydispersity indices (PDIs) [5-9]. Polylactide has applications in biomedical, packaging, tissue engineering, and pharmaceutical fields [9-12]. Therefore, using initiators based on complexes containing biologically benign metals are important. In this regard, initiators based on alkali metals [13], magnesium [14,15], calcium [16,17], zinc [18–20], iron [21], and aluminium [22,23] have been used for the ring-opening polymerisation (ROP) of LA, with promising results. However, there have been few studies regarding the use of Cu(II)-based initiators [24-30], and those reported polymerised LA with low activities and stereoselectivities and required high temperatures. Recently, (*nacnac*^{Bn}CuO*i*Pr)$_2$ showed unusually high activity with low heteroselectivity (P_r = 0.56) for the ROP of LA [31]. More recently, diimino pyrrolide copper alkoxide yielded isotactic PLA with high M_n (44–45 kg/mol) and narrow PDIs (1.0–1.2) [32]. Similarly, our group demonstrated that Cu(II) initiators bearing ligands such as *N*1,*N*^{1}-dimethyl-*N*^{2}-[(1*R*)-myrtenylmethyl]ethane-1,2-diamine [33], *N*,*N*-dimethylethylenamine-camphorylimine [34], *N*-(pyridin-2-ylmethyl)amine [35] and (*R*,*R*)-1,2-diaminocyclohexane derivatives effectively catalysed the ROP of *rac*-lactide (*rac*-LA) in a controlled manner and with high activities and stereoselectivities [36,37].

In continuation of our previous work toward the development of effective and stereoselective Cu(II) catalysts for the ROP of *rac*-LA, we describe herein the synthesis and structural characterisation of Cu(II) complexes bearing *N*-substituted (*S*)-phenylethanamine derivatives and their suitability as catalytic precursors for the polymerisation of *rac*-LA. Furthermore, we sought to investigate the effects of ligand architecture on the catalytic efficacy and stereoselectivity of the synthesised complexes toward the ROP of *rac*-LA.

2. Experimental

2.1. General considerations and materials

All manipulations involved in the synthesis of ligands ($L^1 – L^3$) and their corresponding Cu(II) complexes, $[L^nCuCl_2]_2$ ($L^n = L^1 – L^3$), were performed using bench-top techniques in the air, unless otherwise specified. The synthesis of alkoxide derivatives of the Cu(II) complexes and ROP reactions was performed using standard Schlenk techniques, high vacuum, and glove box under argon. Tetrahydrofuran (THF) was dried over Na/benzophenone ketyl, while CH_2Cl_2 was dried over CaH_2; these solvents were subsequently distilled from these reagents under argon prior to use. The *rac*-lactide (*rac*-LA) was purchased from Aldrich and was sublimed prior to use. $CuCl_2.2H_2O$, 2-pyridinecarboxyaldehyde, pyrazole, 3,5-dimethylpyrazole, (*S*)-phenylethanamine and $LiOCHMe_2$ (2.0 M in THF) were obtained from Aldrich chemical company. NMR solvents were purchased from Sigma Aldrich and stored over 3 Å molecular

sieves. Various solvents such as EtOH, Et_2O, *n*-hexane and MeOH were purchased from high grade commercial suppliers.

2.2. Instrumentation

^1H (operating at 500 MHz) and ^{13}C (operating at 125 MHz) NMR spectra were recorded on a Bruker Avance Digital 500-NMR spectrometer (Bruker, Billerica, MA), and chemical shifts were recorded in ppm units (δ) relative to residual protium in the deuterated solvents ($CDCl_3$, δ = 7.26). Coupling constants were reported in Hertz (Hz). Data was recorded as m = multiplet, br = broad, s = singlet, d = doublet, t = triplet and q = quartet. For the homonuclear decoupling NMR spectroscopy, Bruker Avance digital 600-NMR spectrometer was used. Infrared spectra (IR) (neat) were recorded on Bruker FT/IR-Alpha and the data were reported in cm^{-1}. Elemental analyses were determined using the EA 1108-Elemental Analyzer at the Chemical Analysis Laboratory of the Centre for Scientific Instruments of Kyungpook National University. Gel permeation chromatography (GPC) analyses were carried out on a Waters Alliance GPCV2000, equipped with differential refractive index detectors. The GPC columns were eluted with tetrahydrofuran (THF) with 1 mL/min rate at 25 °C and were calibrated with monodisperse polystyrene standards. The ^1H NMR spectra for examining PLA microstructures in terms of tetrad distributions were recorded in $CDCl_3$ and analysed according to previous studies [38-41].

2.3. Synthesis of ligands

2.3.1. Synthesis of L[1]

A CH_2Cl_2 (10 mL) solution of (*S*)-(-)-methylbenzylamine (2.00 g, 16.50 mmol) was treated with a CH_2Cl_2 (10 mL) solution of (1*H*-pyrazol-1-yl)methanol (1.62 g, 16.50 mmol) at 0 ^oC for 12 h. The reaction mixture was dried over $MgSO_4$ and the solvent was removed *in vacuo* to yield colorless oil as a final product (2.86 g, 86.1%). Anal. Calcd. for $C_{12}H_{15}N_3$: C 71.61; H 7.51; N 20.88, Found: C 71.78, H 7.60, N 21.06 %. ^1H NMR (500 MHz, $CDCl_3$, 298 K) δ = 7.50 (d, J = 1.78 Hz, 1H, pz**H**), 7.27-7.26 (m, 1H, pz**H**), 7.25-7.16 (m, 5H, ph**H**), 6.14 (t, J = 2.02 Hz, 1H, pz**H**), 4.92 (d, J = 13.64 Hz, 1H, C$\boldsymbol{H_a}$$H_b$), 4.54 (d, J = 13.64 Hz, 1H, $CH_a\boldsymbol{H_b}$), 3.45 (q, 1H, J = 6.31 Hz, ph-C**H**-NH), 2.26 (br, 1H, N**H**), 1.20 (d, J = 6.31 Hz , 3H, C$\mathbf{H}_3$). ^{13}C NMR (500 MHz, $CDCl_3$): δ =144.11, 140.08, 129.51, 128.64 (2C, ph**C**), 127.36, 127.08 (2C, ph**C**), 104.92, 63.23, 53.58, 24.46. IR (Neat; oily liquid; cm^{-1}): 3298 (w), 2965 (m), 2867 (w), 1510 (m), 1490 (m), 1451 (s), 1393 (m) 1266 (s), 1226 (w), 1083 (s), 749 (s), 701 (s).

2.3.2. Synthesis of L[2]

An analogous method to that of L^1 was utilized except that CH_2Cl_2 (10 mL) solution of (*S*)-(-)-methylbenzylamine (2.00 g, 16.50 mmol) was treated with CH_2Cl_2 (10 mL) solution of 3,5-dimethyl-1H-pyrazol-1-yl)methanol (2.08 g, 16.50 mmol) at 0 ^oC to yield colorless oil (3.22 g, 84.9%). Anal. Calcd. for $C_{14}H_{19}N_3$: C 73.33; H 8.35; N 18.32, Found: C 73.39, H 8.37, N 18.37 %. ^1H NMR (500 MHz, $CCDl_3$, 298 K) δ = 7.29-7.16 (m, 5H, ph**H**), 5.67 (s, 1H, pz**H**), 4.70 (d, J = 13.64 Hz, 1H, C$\boldsymbol{H_a}$$H_b$), 4.49 (d, J = 13.64 Hz, 1H, $CH_a\boldsymbol{H_b}$), 3.54 (q, 1H, J = 6.56 Hz, ph-C**H**-NH), 2.43 (br, 1H, N**H**), 2.17 (s, 3H, pz-C$\mathbf{H_3}$), 1.85 (s, 3H, pz-C$\mathbf{H_3}$), 1.23 (d, J = 6.56 Hz , 3H, C$\mathbf{H_3}$). ^{13}C NMR (500 MHz, $CDCl_3$): δ = 148.01, 144.57, 139.39, 128.49(2C, ph**C**), 127.11, 126.82 (2C, ph**C**), 104.70, 59.63, 53.59, 24.89, 13.55, 10.51. IR (Neat; oily

liquid; cm^{-1}): 3287 (w), 3028 (w), 2963 (m), 2868 (w), 1551 (s), 1452 (s), 1269 (s), 1029 (s), 762 (s), 701 (s).

2.3.1. Synthesis of L^3

A CH_2Cl_2 solution (20 mL) of (*S*)-methylbenzylamine (3.00 g, 24.75 mmol) and 2-pyridinecarboxaldehyde (3.12 g, 24.75 mmol) was stirred at ambient temperature for 2 days. The reaction mixture was dried over $MgSO_4$ and the solvent was removed *in vacuo*. The imine compound was isolated as yellow sticky oil. $NaBH_4$ (1.30 g, 3.43 mmol) was added to the MeOH (50 mL) solution of imine compound at 0 °C. The solvent was removed *in vacuo* after stirring for one day and the resultant residue was treated with water (40 mL) and CH_2Cl_2 (40 mL). Combined organic phase was separated, dried over $MgSO_4$. The solvent was removed *in vacuo* to yield light yellow oil as a final product (4.36 g, 90 %). Anal. Calcd. for $C_{14}H_{16}N_2$: C 79.21; H 7.60; N 13.20, Found: C 79.30, H 7.65, N 13.24 %. ^{1}H NMR (500 MHz, $CDCl_3$, 298 K) δ = 8.50 (d, J = 4.80 Hz, 1H, py**H**), 7.64 (t, J = 7.83 Hz, 1H, py**H**), 7.48 (d, J = 7.83 Hz, 1H, py**H**), 7.42-7.40 (m, 2H, ph**H**), 7.34-7.31 (m, 2H, ph**H**), 7.25-7.20 (m, 1H, ph**H**), 7.13 (t, J = 6.06 Hz, 1H, py**H**), 3.73 (d, J = 14.40 Hz, 1H, C$\boldsymbol{H_a}$H$_b$), 3.70 (q, J = 6.56 Hz, 1H, ph-C**H**-NH), 3.53 (d, J = 14.40 Hz, 1H, CH$_a$$\boldsymbol{H_b}$), 1.78 (br, 1H, N**H**), 1.44 (d, J = 6.56 Hz, 3H, C$\mathbf{H_3}$). ^{13}C NMR (500 MHz, $CDCl_3$): δ = 159.88, 149.32, 145.44, 136.32, 128.48, 126.97, 126.80, 122.43, 121.85, 58.06, 53.13, 24.47. IR (Neat; oily liquid; cm^{-1}): 3315 (w), 3060 (w), 2965 (w), 1590 (m), 1568 (m), 1491(m), 1473 (m), 1450 (m), 1432 (m), 1369 (m), 1128 (m), 756 (s), 700 (s).

2.4. Synthesis of Cu(II) complexes

2.4.1. Synthesis of $[L^1CuCl_2]$

A CH_2Cl_2 solution (10 mL) of L^1 (0.56 g, 2.78 mmol) and $CuCl_2{\cdot}2H_2O$ (0.47 g, 2.78 mmol) was stirred at ambient temperature for 12 h. The solution of reaction mixture was dried over anhydrous $MgSO_4$ and the organic solvent was reduced under reduced pressure. Washing with Et_2O afforded green solid. The green solid was dried under vacuum at 60 °C to get final product (0.80 g, 88.2%). Anal. Calcd. for $C_{24}H_{30}Cl_4Cu_2N_6$: C 42.93; H 4.50; N 12.52, Found: C 43.00, H 4.54, N 12.56%. IR (solid neat; cm^{-1}): 3223 (w), 3184 (m), 3106 (w), 2965 (w), 1518 (m), 1499 (m), 1452 (s), 1390 (m), 1269 (s), 1196 (m), 1065 (s), 782 (s), 755 (s), 732 (s), 701 (s).

2.4.2. Synthesis of $[L^2CuCl_2]$

An analogous method to that of $[L^1CuCl_2]$ was utilize except that L^2 (0.52 g, 2.26 mmol) was treated with CH_2Cl_2 (30 mL) solution of $CuCl_2{\cdot}2H_2O$ (0.38 g, 2.26 mmol) to afforded green solid as a final product (0.70 g, 87.4%). Anal. Calcd. for $C_{28}H_{38}Cl_4Cu_2N_6$: C 46.22; H 5.26; N 11.55, Found: C 46.27, H 5.24, N 12.00%. IR (solid neat; cm^{-1}): 3162 (w), 2975 (w), 2928 (w), 1552 (s), 1468 (s), 1385 (s), 1290 (m), 1265 (m), 1017 (s), 785 (s), 739 (s), 703 (s).

2.4.3. Synthesis of $[L^3CuCl_2]$

An analogous method to that of $[L^1CuCl_2]$ was utilize except that L^3 (2.58 g, 12.15 mmol) was treated with CH_2Cl_2 (30 mL) solution of $CuCl_2{\cdot}2H_2O$ (2.07 g, 12.15 mmol) $CuCl_2{\cdot}2H_2O$ to afford green solid as a final product (3.81 g, 91 %). Anal. Calcd. for $C_{28}H_{32}Cl_4Cu_2N_4$: C 48.49; H 4.65; N 8.08, Found: C 49.05, H 4.69, N 8.12%. IR (solid neat; cm^{-1}): 3202 (m), 3171 (m), 3070 (w) 2943 (w), 1606 (m), 1571 (m), 1482 (m), 1444 (m), 1420 (m), 1379 (m), 1289 (m), 1104 (m), 1053 (m), 1027 (s), 767 (s), 695 (s).

2.5. X-ray Crystallography

An X-ray quality single crystals of $[L^nCuCl_2]$ ($L^n = L^1$ - L^3) were mounted in a thin-walled glass capillary on an Enraf-Noius CAD-4 diffractometer with Mo Kα radiation (λ = 0.71073 Å). Unit cell parameters were determined by least-squares analysis of 25 reflections (11° < θ < 14°). Intensity data were collected with θ range of 1.56° – 25.47° in ω/2θ scan mode. Three standard reflections were monitored every 1 h during data collection. The data was corrected for Lorentz-polarization effects and decay. Empirical absorption corrections with *ψ*-scans were applied to the data. The structure was solved by using Patterson method and refined by full-matrix least-squares techniques on F^2 using *SHELXL*-97 [42] and *SHELXSL* program packages [43]. All non-hydrogen atoms were refined anisotropically and all hydrogen atoms were positioned geometrically using a riding model with fixed isotropic thermal factors. Structural refinement and crystallographic data for $[L^nCuCl_2]_2$ ($L^n = L^1 – L^3$) is presented in **Table 1**.

2.6. Polymerisation studies

Alkoxide derivatives were prepared *in situ* by adding a THF solution of $LiOCHMe_2$ (0.50 mL of 2.0 *M* solution of in THF, 1.00 mmol) dropwise to a THF (7.50 mL) solution of Cu(II) complex (0.50 mmol) at -78 °C. After being stirred for 2 h at room temperature, the resulting THF solution of alkoxide derivatives was used as a catalyst for polymerisation reaction. The general procedure for the ROP of *rac*-LA was as follows. A 100 mL of Schlenk flask was charged with *rac*-LA (0.90 g, 6.25 mmol) in the glove box. Dried CH_2Cl_2 (5 mL) was transferred to the reaction vessel *via* syringe and stirred to make a clear solution. The reaction was initiated by quickly adding the catalyst solution (1.00 mL, 0.0625 mmol) *via* a gas tight syringe under argon in the monomer solution at 25 °C. Then the reaction mixture was stirred at 25 °C for specified time. The polymerisation reaction was quenched after 3 min using H_2O (3 mL) and sequentially precipitated by adding hexane (20 mL). The resultant sticky polymeric material was dried *in vacuo* and the obtained fluffy solid was subjected to ^{1}H NMR analysis. ^{1}H NMR (400 MHz, $CDCl_3$, 298 K): *δ* 5.14–5.25 (m, 1H), 1.54–1.63 (m, 3H). Conversion yield was determined by observing the methine resonance integration of monomer *vs.* polymer methyl resonances in the ^{1}H NMR spectra.

3. Results and Discussion

3.1. Synthesis

The ligands (*S*)-*N*-((1H-pyrazol-1-yl)methyl)-1-phenylethanamine (L^1) and (*S*)-*N*-((3,5-dimethyl-1H-pyrazol-1-yl)methyl)-1-phenylethanamine (L^2) were obtained *via* a single step condensation reaction of (*S*)-phenylethanamine with (1H-pyrazol-1-yl)methanol and (3,5-dimethyl-1H-pyrazol-1-yl)methanol, respectively, in CH_2Cl_2. However, for (*S*)-1-phenyl-*N*-

((pyridin-2-yl)methyl)ethanamine (L^3), the condensation reactions of (*S*)-phenylethanamine with corresponding 2-pyridinecarboxyaldehyde yielded the imine intermediate, which was sequentially reduced to the amine using a mild reducing agent, i.e. $NaBH_4$ (**Scheme 1**). The structure and identity of the ligands were characterised using ^1H nuclear magnetic resonance (^1H NMR) and ^{13}C NMR spectroscopies. The methine protons Ph–C**H**–CH_3 appeared at δ = 3.45, 3.54, and 3.70 ppm in L^1, L^2, and L^3, respectively. Similarly, the C**H**$_3$ protons appeared at 1.20 for L^1, 1.23 for L^2, and 1.44 ppm for L^3. The corresponding $[L^nCuCl_2]_2$ (L^n = L^1–L^3) complexes were obtained (88–91% yields) by direct ligation of the metal-containing starting materials with the ligands in the 1:1 ratio in dry CH_2Cl_2 at ambient temperature (**Scheme 1**). Owing to the paramagnetic nature of the Cu(II) complexes, we were unable to structurally characterise the $[L^nCuCl_2]_2$ (L^n = L^1–L^3) *via* NMR spectroscopy. However, the infrared spectra of the ligands in the N–H stretching region were compared with those of the complexes. Characteristic N–H peaks for L^1, L^2, and L^3 were observed at 3298, 3287, and 3315 cm^{-1}, whereas the N–H stretching bands appeared at 3223, 3162, and 3203 cm^{-1} in the corresponding Cu(II) complexes. Elemental analyses of the synthesised complexes were consistent with the proposed structures shown in **Scheme 1** and confirmed the purity of the isolated complexes $[L^nCuCl_2]_2$ (L^n = L^1–L^3). All of the synthesised complexes were stable toward oxygen and moisture.

3.2. Molecular structure

X-ray quality single crystals of $[L^nCuCl_2]_2$ (L^n = L^1–L^3) were obtained by layering *n*-hexane on CH_2Cl_2 solutions. Their molecular structures at the 30% probability level are illustrated in **Figs**. **1–3**, respectively. The representative bond lengths and angles are listed in **Table 2**. The synthesised Cu(II) complex $[L^1CuCl_2]_2$ crystallised in the orthorhombic system with space group $P2_12_12_1$, whereas $[L^2CuCl_2]_2{\cdot}2CH_2Cl_2$ and $[L^3CuCl_2]_2$ crystallised in the monoclinic system with space group $P2_1$.

It is evident from the molecular structures that the Cu atom in each independent unit adopted a distorted square planar geometry by coordinating with two nitrogen atoms of the

bidentate ligand in a chelating manner and with one terminal and one bridging chloro ligand. The $Cu–N_{amine}$ bond distances varied from 2.086(3) to 2.0793(3) Å in $[L^1CuCl_2]_2$, 2.072(3) to 2.104(3) Å in $[L^2CuCl_2]_2$ and 2.022(3) to 1.999(2) Å in $[L^3CuCl_2]_2$. Similarly, the $Cu–N_{pyrazole}$ bond lengths were 1.961(4) and 1.963(4) Å for $[L^1CuCl_2]_2$ and 1.977(4) and 1.984(4) Å for $[L^2CuCl_2]_2$, whereas the $Cu–N_{pyridine}$ lengths were 2.003(2) and 1.999(2) Å for $[L^3CuCl_2]_2$. These $Cu–N_{amine}$ and $Cu–N_{pyrazole/pyridine}$ bond lengths are in the expected range for complexes with similar ligands [35,44]. It is evident that the pyrazole substituents influenced the $Cu–N_{pyrazole}$ bond lengths. Ligands with the bulkier pyrazole moiety in $[L^2CuCl_2]_2$ led to longer bond lengths compared with the $[L^1CuCl_2]_2$ analogue having an unsubstituted pyrazole moiety. The $Cu–Cl_{terminal}$ bond lengths ranged from 2.231(9) to 2.275(12) Å in $[L^nCuCl_2]_2$ ($L^n = L^1–L^3$); they were shorter than the Cu1–Cl1 and Cu2–Cl4 bond lengths, which ranged from 2.2620(11) to 2.2702(19) Å. However, the $Cu–Cl_{terminal}$ lengths lay in the range reported for related complexes [35,45]. The Cu1···Cl4 and Cu2···Cl2 bond lengths, ranging from 2.745(2) to 2.818 Å in the $[L^nCuCl_2]_2$ ($L^n = L^1–L^3$) complexes, are consistent with weak interactions; the lengths were slightly affected by the substituents attached to the pyrazole moiety (**Table 2**). All of the synthesised complexes had a Cu···Cu separation averaging 3.435(7) Å. This length is shorter than that previously reported for complexes having the same ligand framework [35, 46].

The average $N_{amine}–Cu–N_{pyrazole/pyridine}$ bond angles in $[L^1CuCl_2]_2$, $[L^2CuCl_2]_2$, and $[L^3CuCl_2]_2$ ranged from 80.37(13) to 82.49(10)°, revealing the distortion from ideal square planar geometry. Distortion from the ideal geometry is also evident from the dihedral angle between the Cl2–Cu–Cl1 and $N_{pyrazole/pyridine}–Cu–N_{amine}$ planes, which ranged from 11.8(2)° to 19.8(2)°. Similarly, the $N_{pyrazole}–Cu–Cl_{terminal}$ angles are 94.7(1)° and 94.8(1)° in $[L^1CuCl_2]_2$, 98.3(1)° and 97.5(1)° in $[L^2CuCl_2]_2$, 96.05(8)° and 95.67(8)° in $[L^3CuCl_2]_2$ and are found to be are smaller than those of our previously reported complexes (Table 3) [35,45]. The $N_{pyrazole}–Cu–Cl_{terminal}$ angles were slightly affected by pyrazole/pyridine moieties. The $Cl_1–Cu1–Cl_2$ bite angles were 94.04(5)°, 93.92(4)° and 92.46(4)°, whereas the $Cl_3–Cu2–Cl_4$ angles were 94.11(5)°, 92.46(4)° and 93.21(3)° in $[L^1CuCl_2]_2$, $[L^2CuCl_2]_2$ and $[L^3CuCl_2]_2$, respectively.

The formation of Cu(II) complexes by ligation of *N*-substituted phenylethanamine ligands containing a stereogenic carbon centre (derived from (*S*)-methylbenzylamine) induced chirality in the nitrogen atoms of the pyrazole and pyridine moieties by restricting free motion [47-49]. It is evident from the molecular structures that the induced chirality of the nitrogen atom in the same crystal structure is different. For example, $[L^nCuCl_2]_2$ exists as a dimer with two molecules in asymmetric units in the (S_C, S_N) and (S_C, R_N) configuration (**Figs. 1–3**). Wang et al. reported a compound containing camphor-based ligands in which the asymmetric unit of the compound comprised two diastereomers [50]. These compound represents a very rarely seen example of a four-coordinate dimeric Cu(II) complex having a diastereomeric asymmetric unit.

3.3. *rac*-LA polymerisation

The alkoxide derivatives of the synthesised Cu(II) complexes [$L^nCu(O^iPr)_2$] ($L^n = L^1$–L^3) were investigated for the ROP of *rac*-LA. The polymerisation was carried out at room temperature in CH_2Cl_2. The polymerisation data are listed in **Table 4**. It is evident that the ROP of *rac*-LA was effectively initiated by the alkoxide derivatives, i.e. [$L^nCu(O^iPr)_2$] ($L_n = L^1$–L^3), yielding PLAs with high M_n and narrower PDIs. Complete conversion of *rac*-LA to PLA was confirmed by the absence of monomer (*rac*-LA) signals in the ^{1}H NMR spectra of the resultant PLAs. The polymerisation data in **Table 4** establish that the conversion of monomer to polymer was complete within 2 min using the [$L^nCu(O^iPr)_2$] ($L_n = L^1$ and L^3) initiators, whereas the [$L^2Cu(O^iPr)_2$] initiator effected complete polymerisation within 3 min (**Table 4**).
The M_n of the PLAs made using [$L^nCu(O^iPr)_2$] ($L^n = L^1$–L^3) were determined based on using ^{1}H NMR end-group analysis and by GPC in THF relative to polystyrene standards [51]. The M_n determined from the ^{1}H NMR spectra of the obtained polymer and those determined with GPC for the alkoxide derivatives of the Cu(II) initiators were almost identical to the M_n (corrected using the Mark–Howink factor of 0.58) [52] value calculated from the monomer/initiator molar ratio. The M_n of PLA determined by GPC are typically larger than the actual molecular weights, when using polystyrene standards for GPC analysis of PLA. In order to compensate such discrepancies, multiplication of the GPC data by a factor of 0.58 has been recommended to attain more accurate M_n [53-55]. The experimentally determine M_n values were in good agreement with theoretical M_n values, calculated for one growing polymer chain per initiator molecule. In addition, the narrower PDIs (1.20–1.30) revealed that the polymerisation was well-controlled. Notably, the activities of the Cu(II) initiators in the current study decreased with increasing size of the substituent on the amine moiety. Polymerisation using [$L^2Cu(O^iPr)_2$], bearing dimethyl substituents at the 3 and 5 positions of the pyrazole moiety, was slower than with [$L^1Cu(O^iPr)_2$], bearing the unsubstituted pyrazole moiety (**Table 4**). That complexes with bulkier ligands were less active toward LA polymerisation is attributed to bulky ligands tending to hamper the coordination/insertion of an incoming monomer, which is detrimental to the catalytic activity [56].

End-group analysis by ^{1}H NMR spectroscopy revealed the hydroxyl group [–CHMe–(OH)] signal at δ2.90 ppm; the signals for the isopropoxide [–C(O)CH$(CH_3)_2$] group at the other terminus overlapped with those of the PLA backbones. The ROP of *rac*-LA using these initiators favours a coordination-insertion mechanism [57,58]. In this mechanism, initial coordination of *rac*-LA to the central metal, yielding a penta-coordinated intermediate, is followed by cleavage of the acyl-oxygen bond to open the LA ring. Another molecule of *rac*-LA is opened by attachment to the metal centre in an identical manner. Subsequent addition of *rac*-LA produces hetero-enriched PLA.

Polymerisation with Me_2CHOLi alone was also attempted; the polymeric product was obtained slowly with insignificant stereoselectivity (**Table 4**). The polymerisation data reveal the role of the Lewis acidic metal centre and the influence of the ligand architecture that provided better control over polymerisation and influenced the microstructures of the resultant PLAs. Similarly, the dichloro complexes [$L^nCuCl_2]_2$ ($L^n = L^1$–L^3) showed no activity toward ROP of *rac*-LA under similar experimental conditions.

Microstructural analysis of the obtained PLAs was performed by inspecting the methine proton region of the homodecoupled ^{1}H NMR spectra and *P*r values were calculated with

equation *P*r = 2I1/(I1 + I2), where I1 = (sis + sii) and I2 = (iis + iii + isi), as reported previously [41,59,60]. A representative homodecoupled ^{1}H NMR spectrum of methine region of obtained PLA has been shown in **Fig. 4**. It is evident from the polymerisation data that all of the complexes gave heterotactic PLAs (**Table 4)**. Unlike the catalytic activities, the heterotactic enchainment was not significantly affected by the steric bulk of the ligands around the metal centre. However, it was observed that 3,5-dimethyl-substituted pyrazole-bearing ligands attached to the metal centre exhibited slightly higher heterotactic bias, indicating that large steric hindrance might assist the regularity of monomer insertion.

Compared with our previously reported dimeric Cu(II) complexes, the current system is superior in terms of activity as well heterotacticity [35]. Similarly, unsymmetrical formamidine dimeric Cu(II) complexes exhibited lower activities toward ROP of *rac*-LA compared with our current system, resulting in PLAs with broad PDIs (1.78–1.87) [61]. Imino phenoxide-based copper complexes reported by Mandal et al. for the ROP of LA yielded PLAs with moderate molecular weights with low stereoselectivity at a conversion rate of approximately 90% [62]. Recently reported Nacnac^{Bn}CuO^{i}Pr, proved to be highly active catalyst for ROP of LA but essentially produced atactic PLA [31]. The ligand architecture and pendent groups strongly influence the reactivity and stereo-chemical outcomes in ROP of *rac*-LA. As evident from our previous reports where CuII) ligated to *N*,*N*-dimethylethylenamine-camphorylimine [(CDM)Cu(O^{i}Pr$_2$)$_2$] [34] and N^1,N^1-dimethyl-N^2-[(1*R*)-myrtenylmethyl]ethane-1,2-diamine [(L)Cu(O^{i}Pr$_2$)$_2$] [35] ligands have almost identical backbone and methyl substituents with the only difference of *R*-myrentyl and *R*-camphor pendent groups, exhibited variable activities and stereoslectivities. Thus, the activity as well stereoselectivity for ROP of *rac*-LA can be control by the proper complexity of the substituents at the donor nitrogen atoms of *N*,*N*-bidentate ligands.

The polymerisation results of our current catalytic system show that the activities of these initiators were affected by the steric hindrance provided by the ligand framework around the metal centre. Increased steric bulk around the metal centre negatively affected the activities, whereas the stereoslectivities toward ROP of *rac*-LA remained unaffected. Our results are consistent with polymerisation progressing through a chain-end mechanism, as reported previously [63].

4. Conclusion

We investigated the synthesis and X-ray crystallographic structures of [L^{n}CuCl$_2$]$_2$ (L^n = L^1–L^3) comprising chiral *N*-substituted phenylethanamine derivatives. The molecular structures revealed that the Cu(II) complexes favoured a distorted square planar geometry and existed as dimers in the solid state. The two asymmetric units were diastereomeric with (S_C, S_N) and (S_C, R_N) configurations. The alkoxide derivatives, generated *in situ*, of the Cu(II) complexes exhibited higher activities toward ROP of *rac*-LA and afforded heterotactic PLAs. Steric bulk around the

metal centre negatively affected the polymerisation activity, whereas the resultant stereoselectivity remained unchanged.

Supplementary materials

CCDC 1883665-1883667 contains the supplementary crystallographic data for complexes **[**$L^1CuCl_2]_2$, $[L^1CuCl_2]_2$ and $[L^1CuCl_2]_2$, respectively. These data can be obtained free of charge *via* http://www.ccdc.cam.ac.uk/conts/retrieving.html, or from the Cambridge Crystallographic Data Centre, 12 Union Road, Cambridge CB2 1EZ, UK; fax: (+44) 1223-336-033; or e-mail: deposit@ccdc.cam.ac.uk.

Acknowledgments

This research was supported by Basic Science Research Program through the National Research Foundation of Korea (NRF-2017R1D1A3B03030670).

References

[1] M. Singhvi, D. Gokhale, RSC Adv. 3 (2013) 13558.

[2] S. Mecking, Angew. Chem., Int. Ed. 43 (2004) 1078.

[3] A. Arbaoui, C. Redshaw, Polym. Chem. 1 (2010) 801.

[4] T.A. Hottle, M.M. Bilec, A.E. Landis, Polym. Degrad. Stab. 98 (2013) 1898.

[5] A. Hamitou, T. Ouhadi, R. Jerome, P. Teyssié, J. Polym. Sci: Polym. Chem. Ed. 15 (1977) 865.

[6] H.R. Kricheldorf, T. Mang, J.M. Jonte, Macromolecules 17 (1984) 2173.

[7] J. Wu, T.-L. Yu, C.-T. Chen, C.-C. Lin, Coord. Chem. Rev. 250 (2006) 602.

[8] C.A. Wheaton, P.G. Hayes, B.J. Ireland, Dalton Trans. (2009) 4832.

[9] R.H. Platel, L.M. Hodgson, C.K. Williams, Polym. Rev. 48 (2008) 11.

[10] G.L. Gregory, E.M. López-Vidal, A. Buchard, Chem. Comm. 53 (2017) 2198.

[11] C. Bakewell, A.J.P. White, N.J. Long, C.K. Williams, Angew. Chem. Int. Ed. 53 (2014) 9226.

[12] O.D. Cabaret, B. Martin-Vaca, D. Bourissou, Chem. Rev. 104 (2004) 6147.

[13] D. Alhashmialameer, N. Ikpo, J. Collins, L.N. Dawe, K. Hattenhauer, F.M. Kerton, Dalton Trans. 44 (2015) 20216.

[14] K. Devaine-Pressing, J.H. Lehr, M.E. Pratt, L.N. Dawe, A.A. Sarjeant, C.M. Kozak, Dalton Trans. 44 (2015) 12365.

[15] Y. Wang, W. Zhao, D. Liu, S. Li, X. Liu, D. Cui, X. Chen, Organometallics 31 (2012) 4182.

[16] S. Range, D.F.J. Piesik, S. Harder, Eur. J. Inorg. Chem. (2008) 3442.

[17] H.Y. Chen, L. Mialon, K.A. Abboud, S.A. Miller, Organometallics 31 (2012) 5252.

[18] Y.F. Al-Khafaji, M.R. J. Elsegood, J.W.A. Frese, C. Redshaw, RSC Adv. 7 (2017) 4510.

[19] X.X. Zheng, C. Zhang, Z.X. Wang, J. Organomet. Chem. 783 (2015) 105.

[20] M.J. Walton, S.J. Lancaster, J.A. Wright, M.R.J. Elsegood, C. Redshaw, Dalton Trans. 43 (2014) 18001.

[21] Y.Y. Fang, W.J. Gong, X.J. Shang, H.X. Li, J. Gao, J.P. Lang, Dalton Trans. 43 (2014) 8282.

[22] N. Spassky, M. Wisniewski, C. Pluta, A. Le Borgne, Macromol. Chem. Phys. 197 (1996) 2627.

[23] C.Y. Li, D.C. Liu, B.T. Ko, Dalton Trans. 42 (2013) 11488.

[24] A. John, V. Katiyar, K. Pang, M.M. Shaikh, H. Nanavati, P. Ghosh, Polyhedron 26 (2007) 4033.

[25] L.L. Chen, L.Q. Ding, C. Zeng, Y. Long, Q.X. Lu, J.R. Song, D.D. Fan, J.W. Jin, Appl. Organomet. Chem. 25 (2011) 310.

[26] R.R. Gowda, D. Chakraborty, J. Mol. Catal. A Chem. 349 (2011) 86.

[27] D. Appavoo, B. Omondi, I.A. Guzei, J.L.V. Wyk, O. Zinyemba, J. Darkwa Polyhedron 69 (2014) 55.

[28] A. Routaray, N. Nath, T. Maharana, A.K. Sutar, J. Macromol. Sci. Pure Appl. Chem. 52 (2015) 444.

[29] C.Y. Li, S.J. Hsu, C.l. Lin, C.Y. Tsai, J.-H. Wang, B.T. Ko, C.H. Lin, H.Y. Huang, J. Polym. Sci, Part A: Polym. Chem. 51 (2013) 3840.

[30] S. Fortun, P. Daneshmand, F. Schaper, Angew. Chem. Int. Ed. 54 (2015) 13669.

[31] T.J.J. Whitehorne, F. Schaper, Chem. Commun. 48 (2012) 10334.

[32] S. Fortun, P. Daneshmand, F. Schaper, Angew. Chem. Int. Ed. 54 (2015) 13669.

[33] M.K. Chun, J. Cho, S. Nayab, J.H. Jeong, Bull. Kor. Chem. Soc. 38 (2017) 1527.

[34] K.S. Kwon, S. Nayab, J.H. Jeong, Polyhedron 130 (2017) 23.

[35] S.H. Ahn, M.K. Chun, E. Kim, J.H. Jeong, S. Nayab, H. Lee, Polyhedron 127 (2017) 51.

[36] J. Cho, S. Nayab, J.H. Jeong, Polyhedron 113 (2016) 81.

[37] J. Cho, G. H. Lee, S. Nayab, J.H. Jeong, Polyhedron 99 (2015) 198.

[38] J.E. Kasperczyk, Macromolecules 28 (1995) 3937.

[39] J.E. Kasperczyk, Polymer 40 (1999) 5455.

[40] F. Drouin, T.J.J. Whitehorne, F. Schaper, Dalton Trans. 40 (2011) 1396.

[41] M.T. Zell, B.E. Padden, A.J. Paterick, K.A.M. Thakur, R.T. Kean, M.A. Hillmyer, E.J. Munson, Macromolecules 35 (2002) 7700.

[42] G.M. Sheldrick, Acta Crystallogr. Sect. A 64 (2008) 112.

[43] G.M. Sheldrick, Acta Crystallogr. Sect. C71 (2015) 3.

[44] E. Budzisz, I.-P. Lorenz, P. Mayer, P. Paneth, L. Szatkowski, U. Krajewska, M. Rozalski, M. Miernick, New J. Chem. 32 (2008) 2238.

[45] C. J. Vincent, I. D. Giles, .R. Deschamps, ActaCryst. (2018). E 74, 357.

[46] H. Cho, M.J. Jung, J. Jeon, H. Lee, S. Nayab, Inorg. Chimi. Acta 487 (2019) 221.

[47] S.E. Song, Q.T. Nguyen, J.J. Yu, H.I. Lee, J.H. Jeong, Polyhedron 67 (2014) 264.

[48] D.A. Evans, D. Seidel, J. Am. Chem. Soc. 127 (2005) 9958.

[49] D.A. Evans, S. Mito, D. Seidel, J. Am. Chem. Soc. 129 (2007) 11583.

[50] C. Wang, J. Wu, Acta Cryst. E68 (2012) o93.

[51] H.-Y. Chen, J. Zhang, C.-C. Lin, J.H. Reibenspies, S.A. Miller, Green Chem. 9 (2007) 1038.

[52] M.M. Sava, M. Schappacher, A. Soum, Macromol. Chem. Phys. 203 (2002) 889.

[53] A. Kowalski, A. Duda, S. Penczek, Macromolecules 31 (1998) 2114.

[54] H. Ma, J. Okuda, Macromolecules 38 (2005) 2665.

[55] M.A. Masuelli. J. Polym. & Biopolym. Phys. Chem. 2 (2014) 37.

[56] U. Herber, K. Hegner, D. Wolters, R. Siris, K. Wrobel, A. Hoffmann, C. Lochenie, B. Weber, D. Kuckling, S. Herres-Pawlis, Eur. J. Inorg. Chem. (2016) 4723.

[57] H.R. Kricheldorf, S.R. Lee, S. Bush, Macromolecules 29 (1996) 1375.

[58] N. Ajellal, D.M. Lyubov, M.A. Sinenkov, G.K. Fukin, A.V. Cherkasov, C.M. Thomas, J.F. Carpentier, A.A. Trifonov, Chem. Eur. J. 14 (2008) 5440.

[59] M. Cheng, A.B. Attygalle, E.B. Lobkovsky, G.W. Coates, J. Am. Chem. Soc. 121 (1999) 11583.

[60] B.M. Chamberlain, M. Cheng, D.R. Moore, T.M. Ovitt, E.B. Lobkovsky, G.W. Coates, J. Am. Chem. Soc. 123 (2001) 3229.

[61] W.A. Munzeiwa, V.O. Nyamori, B. Omondi, Appl. Organometal. Chem. (2018) DOI.org/10.1002/aoc.4247

[62] M. Mandal, K. Oppelt, M. List, I. Teasdale, D. Chakraborty, U. Monkowius, Monatsh Chem. 147 (2016) 1883.

[63] D.J. Darensbourg, O. Karroonnirun, Inorg. Chem. 49 (2010) 2360.

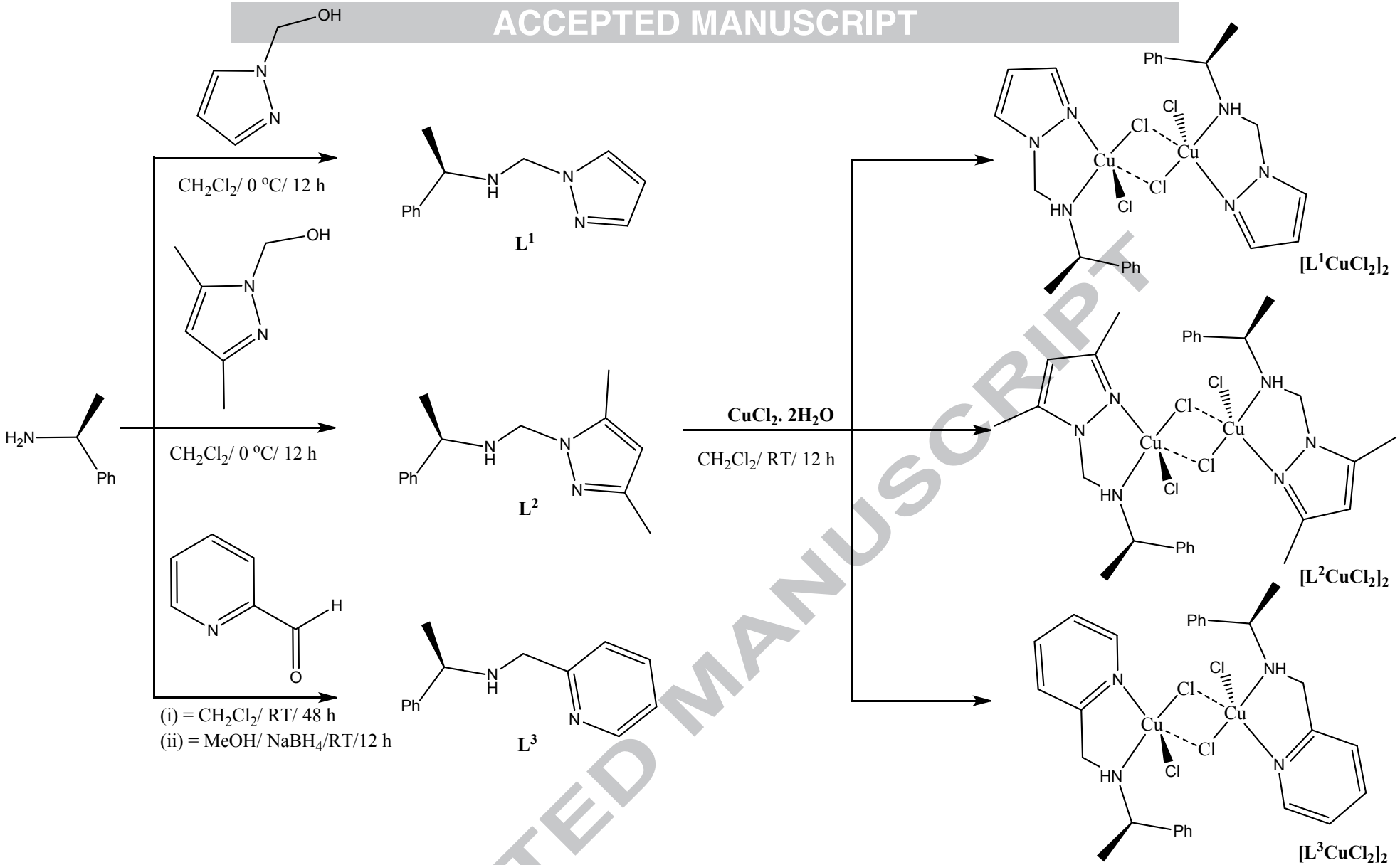

Scheme 1. Synthetic route of chiral *N*-substituted phenylethanamine derivatives and corresponding Cu(II) complexes.

Table 1. Crystal data and structure refinement for $[L^nCuCl_2]_2$ ($L^n = L^1 - L^3$) complexes.

	$[L^1CuCl_2]_2$	$[L^2CuCl_2]_2 \cdot 2CH_2Cl_2$	$[L^3CuCl_2]_2$
Empirical formula	$C_{24}H_{30}Cl_4Cu_2N_6$	$C_{28}H_{38}Cl_4Cu_2N_6 \cdot 2CH_2Cl_2$	$C_{28}H_{32}Cl_4Cu_2N_2$
Formula weight (g/mol)	671.42	897.37	693.46
Wavelength (Å)	0.71069	0.71069	0.71306
Crystal system, Space group	Orthorhombic, $P2_12_12_1$	Monoclinic, $P2_1$	Monoclinic, $P2_1$
Unit cell dimensions			
a (Å)	12.0544(1)	11.481(8)	10.0923(7)
b (Å)	13.3826(1)	9.941(7)	13.1533(8)
c (Å)	17.5951(9)	17.913(6)	11.6087(7)
β (°)	90	102.367(5)	98.109(7)
V (Å^3) , Z	2737.9(4), 2	1997(2), 2	1525.61(17), 2
Dcalc (Mg/m^3)	1.571	1.492	1.510
Absorption coefficient (mm^{-1})	1.900	1.603	1.769
F(0 0 0)	1368	916	708
θ range for data collection (°)	1.91 - 25.47	1.16 - 25.46	1.77- 25.47
Crystal size (mm)	0.50 x 0.50 x 0.45	0.50 x 0.45 x 0.40	0.50 x 0.46 x 0.35
Index ranges	$-14 \le h \le 124$, $-6 \le k \le 16$, $-21 \le l \le 21$	$-13 \le h \le 13$, $-12 \le k \le 12$, $-21 \le l \le 21$	$-12 \le h \le 12$, $-15 \le k \le 15$, $-14 \le l \le 14$
Reflections collected	6085	8397	6301
Independent reflections	5271 (Rint = 0.0229)	7358 (Rint = 0.0126)	5639 (Rint t = 0.0259)
Reflections observed (>2σ)	4860	5962	3776
Data Completeness	0.999	0.994	0.999
Refinement method	Full-matrix least-squares on F2	Full-matrix least-squares on F2	Full-matrix least-squares on F2
Data / restraints / parameters	5271 / 0 / 327	7358 / 1 / 421	5639 / 1 / 345
Goodness-of-fit (GOF) on F^2	1.266	1.069	1.071
Final R indices [I >2δ (I)]	R1 = 0.0234 *w*R2 = 0.0706	R1 = 0.0502 *w*R2 = 0.0938	R1 = 0.0300 *w*R2 = 0.0769
R indices (all data)	R1 = 0.0362 *w*R2 = 0.1095	R1 = 0.0502 *w*R2 = 0.1016	R1 = 0.0356 *w*R2 = 0.0793
Absolute structure parameter	0.007(15)	0.002(11)	0.000(10)
Largest diff. peak & hole (e. Å^{-3})	0.249 and -0.293	0.521 and -0.398	0.641 and -0.539

Table 2. Selected bond lengths (Å) and bond angles (°) of synthesised $[L^nCuCl_2]_2$ ($L^n = L^1 – L^3$) complexes.

	$[L^1CuCl_2]_2$	$[L^2CuCl_2]_2$	$[L^3CuCl_2]_2$	
Bond Lengths (Å)				
N(1)-Cu(1)	1.961(4)	1.977(4)	N(1)-Cu(1)	2.003(2)
N(3)-Cu(1)	2.086(3)	2.072(3)	N(2)-Cu(1)	2.023(3)
Cu(1)-Cl(1)	2.257(1)	2.275(1)	Cu(1)-Cl(1)	2.2385(9)
Cu(1)-Cl(2)	2.262(1)	2.270(2)	Cu(1)-Cl(2)	2.2887(8)
Cu(1)-Cl(4)	2.765(1)	2.818(2)	Cu(1)-Cl(4)	2.811(1)
N(4)-Cu(2)	1.963(4)	1.984(4)	N(4)-Cu(2)	2.057(3)
N(6)-Cu(2)	2.079(3)	2.104(3)	N(3)-Cu(2)	1.999(2)
Cu(2)-Cl(4)	2.264(1)	2.269(2)	Cu(2)-Cl(4)	2.2691
Cl(2)-Cu(2)	2.745(1)	2.876(2)	Cl(2)-Cu(2)	2.7698(9)
Cu(2)-Cl(3)	2.231(1)	2.276(1)	Cu(2)-Cl(3)	2.264(1)
Bond Angles (°)				
N(1)-Cu(1)-N(3)	81.6(2)	80.9(2)	N(1)-Cu(1)-N(2)	82.5(1)
N(4)-Cu(2)-N(6)	81.0(2)	80.4(1)	N(3)-Cu(2)-N(4)	81.9(1)
N(1)-Cu(1)-Cl(1)	94.7(1)	98.4(1)	N(1)-Cu(1)-Cl(1)	96.05(8)
N(6)-Cu(2)-Cl(4)	88.7(1)	91.31(9)	N(4)-Cu(2)-Cl(4)	90.07(7)
Cl(1)-Cu(1)-Cl(2)	94.04(5)	93.94(4)	Cl(1)-Cu(1)-Cl(2)	92.92(3)
Cl(3)-Cu(2)-Cl(4)	94.11(5)	92.46(4)	Cl(3)-Cu(2)-Cl(4)	93.21(3)
N(1)-Cu(1)-Cl(2)	161.9(1)	159.3(1)	N(1)-Cu(1)-Cl(2)	164.15(7)
N(4)-Cu(2)-Cl(4)	167.8(1)	164.4(1)	N(3)-Cu(2)-Cl(4)	161.51(8)

Table 3. The comparison of geometric parameters of synthesized dimeric Cu(II) complexes $[L^nCuCl_2]_2$ ($L^n = L^1 – L^3$), with related complexes from literature.

Bond Lengths (Å)

$Cu\text{-}N_{pyrdine}$	$Cu\text{-}_{Pyrazole}$	$Cu–N_{amine}$	$Cu\text{-}Cl_{terminal}$	Complexes	References
-	1.961(4)	2.086(3)	2.257(1)	**$[L^1CuCl_2]_2$**	This work
-	1.977(4)	2.072(3)	2.275(1)	**$[L^2CuCl_2]_2$**	This work
2.003(2)	-	2.023(3)	2.2385(9)	**$[L^3CuCl_2]_2$**	This work
2.012(7)	-	2.038(4)	2.239(2)	**$[(npmb)Cu(\mu\text{-}Cl)Cl]_2$**	[45]
2.000(1)	-	2.069(1)	2.236(9)	**$[L_BCu(\mu\text{-}Cl)Cl]_2$**	[35]
-	2.026(3)	-	2.294(1)	**$[Cu_2Cl_4(C_6H_{10}N_2)_4]$**	[46]
2.092(0)	2.089(1)	-		**$[LCuCl_2]_2$ (5)**	[44]

Bond Lengths (°)

$N_{pyrazole/pyridine}–Cu–N_{amine}$	$N_{pyrazole}–Cu–Cl_{terminal}$	Complexes	References
81.6(2)	94.7(1), 94.8(1)	**$[L^1CuCl_2]_2$**	This work
80.9(2)	98.4(1), 97.5(1)	**$[L^2CuCl_2]_2$**	This work
82.5(1)	96.05(8), 95.67(8)	**$[L^3CuCl_2]_2$**	This work
83.00(5)	97.64(4)	**$[L_BCu(\mu\text{-}Cl)Cl]_2$**	[35]
80.40(3)	94.80(2)	**$[(npmb)Cu(\mu\text{-}Cl)Cl]_2$**	[45]

Table 4. Polymerisation of *rac*-LA with *in situ* generated [$L^nCu(O^iPr)_2$] ($L^n = L^1 – L^3$).

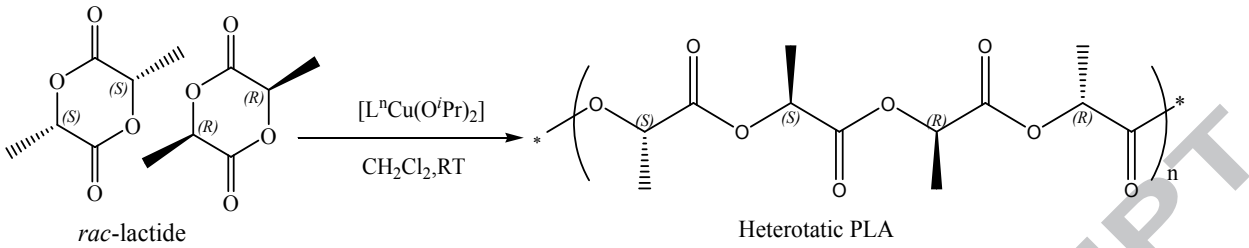

rac-lactide Heterotatic PLA

Run[a]	Catalyst	Time (min)	Conv.[b] (%)	M_n[c] (g/mol) (calcd)	M_n[d] (g/mol) (NMR)	M_n[e] (g/mol) (GPC)	PDI	P_r[f]
1	**$LiOCHMe_2$[g]**	10	100	14,400	15,090	14,030	1.43	0.54
2	**[$L^1Cu(O^iPr)_2$]**	2	100	14,400	14,480	14,110	1.28	0.85
3	**[$L^2Cu(O^iPr)_2$]**	3	100	14,400	14,410	14,250	1.25	0.86
4	**[$L^3Cu(O^iPr)_2$]**	2	100	14,400	14,480	14,750	1.30	0.85

[a]Monomer/catalyst ratio = 100, Solvent CH_2Cl_2 (5.0 mL), room temperature. [b] Monomer conversion was determined by ^{1}H NMR. [c]M_n x10^3(calcd.) was calculated from [molecular weight of *rac*-LA]×[*rac*-LA]/[initiator] ×conversion%. [d] Experimental molecular weight determined by the relative intensities of the main chain and terminal resonances from ^{1}H-NMR spectra. [e] Experimental values were determined by gel permeation chromatography (GPC) in THF relative to 10 polystyrene standards (corrected using the Mark–Houwink factor of 0.58) [52]. [f] Probability of heterotactic enchainment (P_r) were calculated on the basis of ^{1}H NMR spectra according to literature [41,59,60]. [g] Blank polymerisation solely by $LiOCHMe_2$, monomer/catalyst ratio was kept constant at 100 in 5.0 mL of CH_2Cl_2.

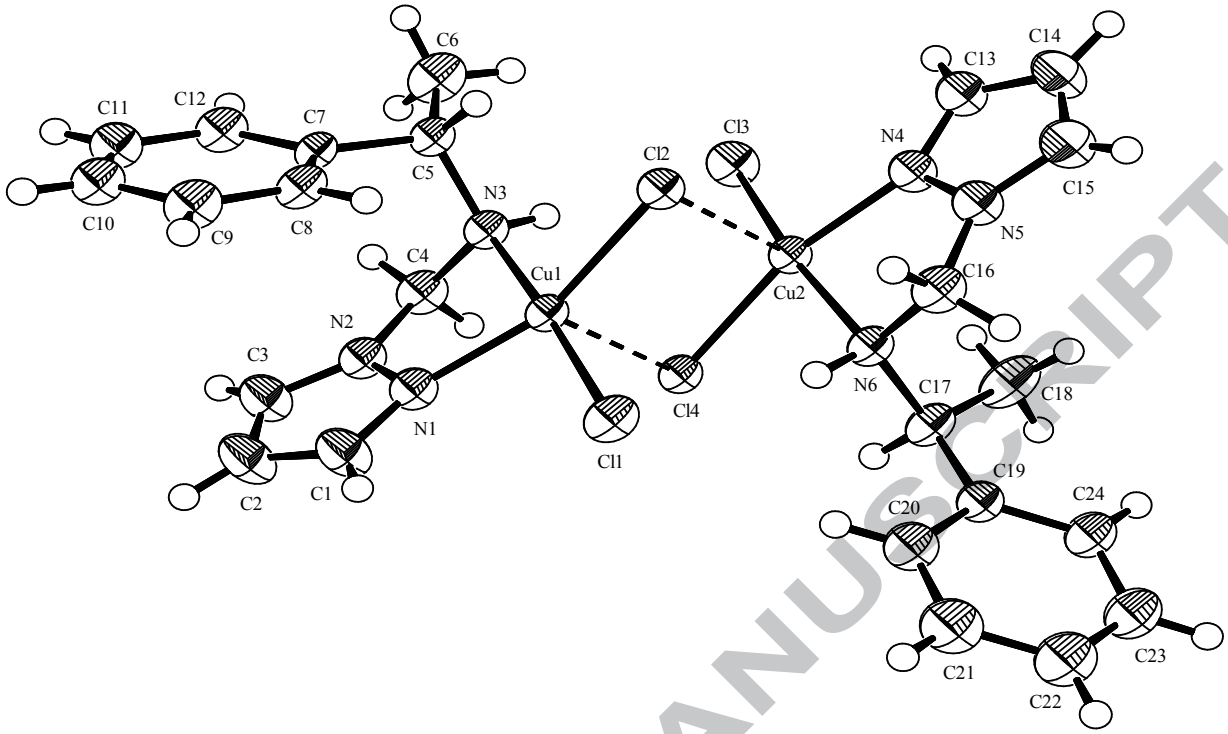

Fig. 1. An ORTEP drawing of $[L^1CuCl_2]_2$ with the numbering scheme at 30% probability level.

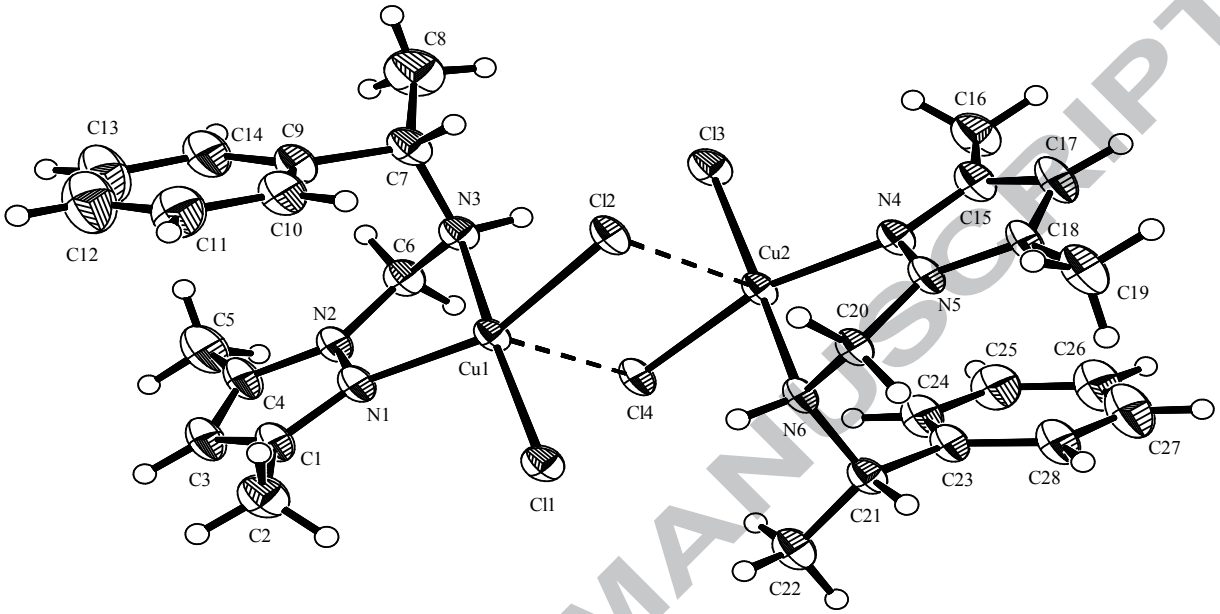

Fig. 2. An ORTEP drawing of **$[L^2CuCl_2]_2$** with the numbering scheme at 30% probability level.

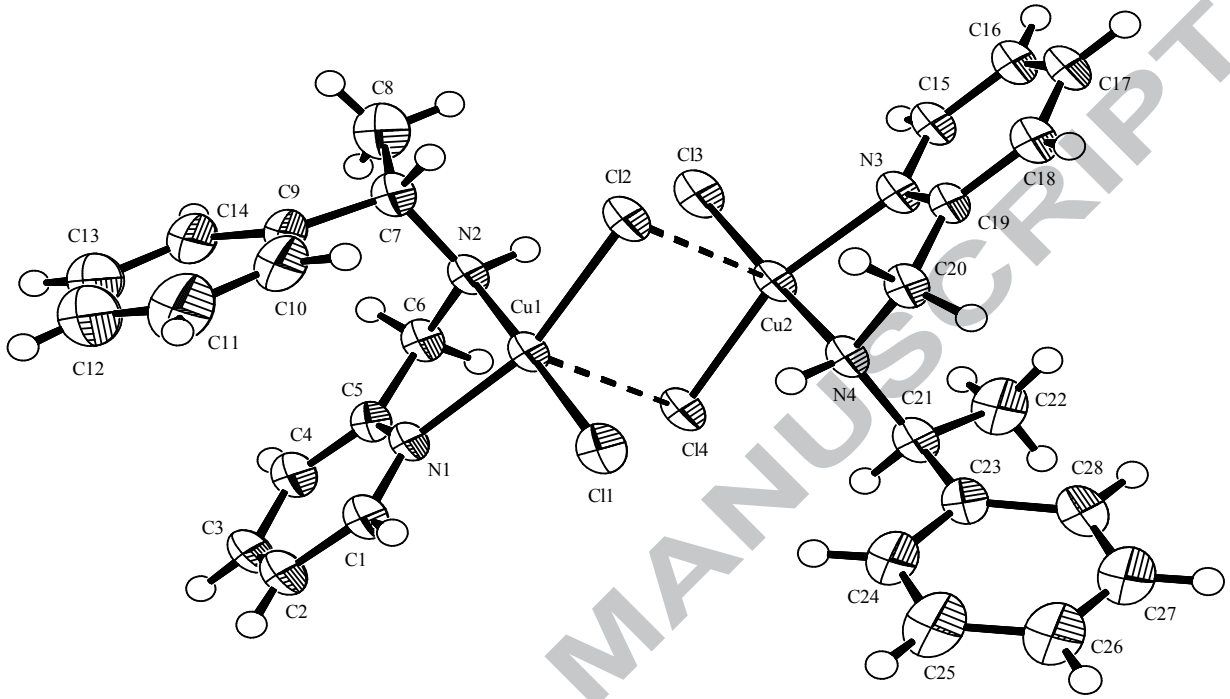

Fig. 3. An ORTEP drawing of $[L^3CuCl_2]_2$ with the numbering scheme at 30% probability level.

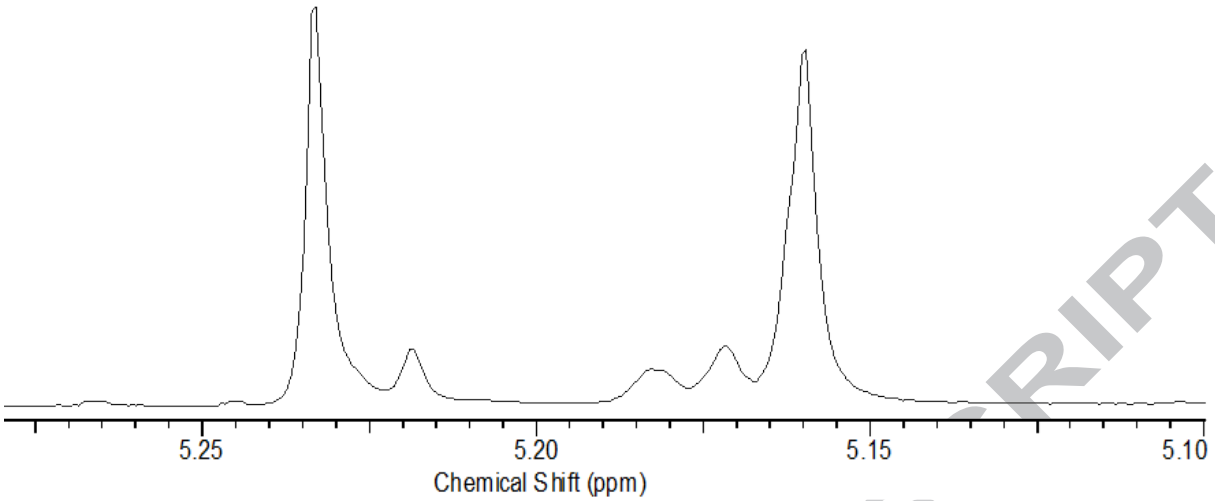

Fig. 4. Homonuclear decoupled ^{1}H NMR spectrum of methine region of heterotactic PLA obtained with **[L^{2}CuO^{i}Pr$_{2}$]** in CH_2Cl_2.

Graphical Abstract (Pictorial)

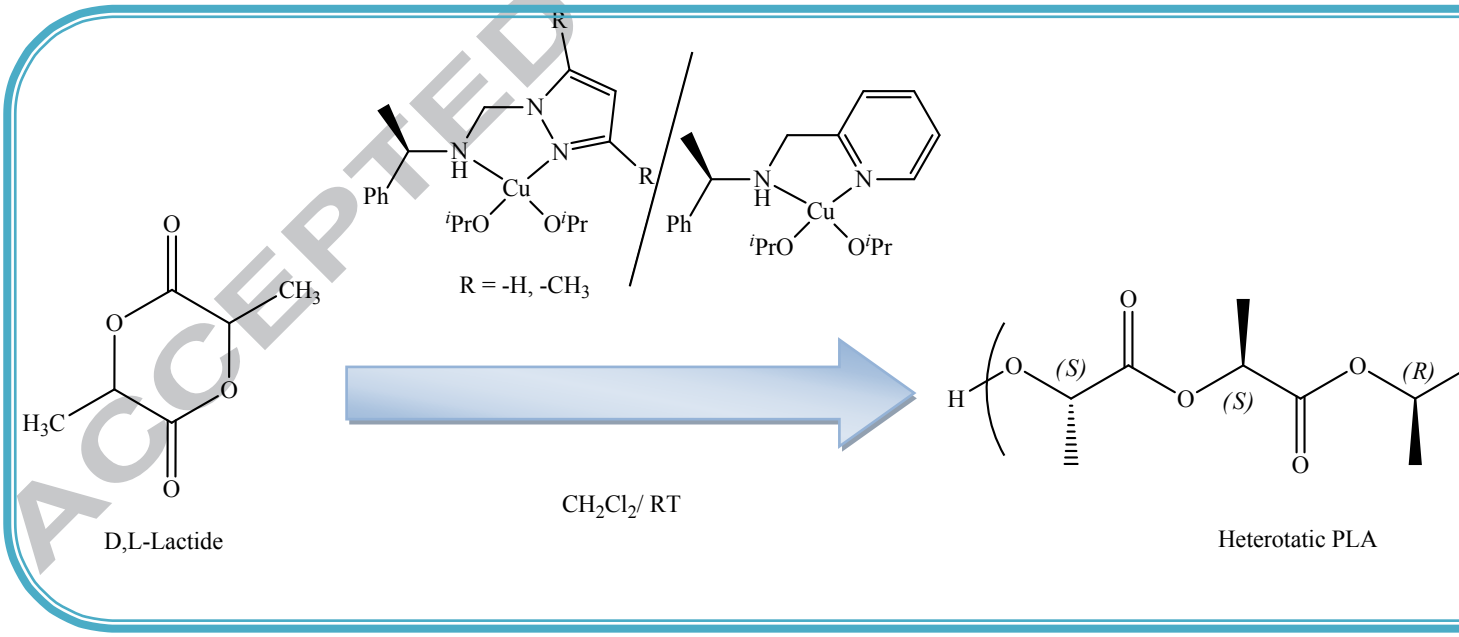

Graphical Abstract (Synopsis)

A series of Cu(II) complexes supported by bearing *N*-substituted phenylethanamine derivatives have been synthesised and characterised by X-ray diffraction. The distorted square planner Cu(II) complexes crystallized in dimeric form with two diastereomeric asymmetric units, i.e. (S_C,S_N and $S_C R_N$). Alkoxy derivatives, generated *in situ*, effectively polymerised *rac*-LA in controlled fashion yielding hetero-enriched PLA (P_r = 0.86). The ROP activity of the current system largely rely on steric hindrance imposed by the substituents attached to ligand architecture.